CHAPTER - 7

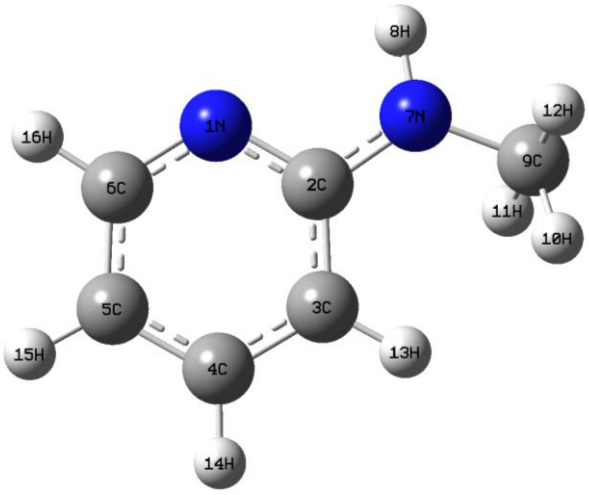

VIBRATIONAL SPECTRAL CHARACTERIZATION OF 2-(METHYLAMINO)PYRIDINE USING HFT CALCULATIONS

CHAPTER - 7

7.1 INTRODUCTION

Azo dyes are a significant class of pyridine derivatives that are broadly engaged as color materials and used for their extraordinary electronic properties as well as their wide color range (Dilellaand, Stidham., 1980; Zerbi, Crawford., 1963; Draeger., 1983). These dyes exhibit azo-hydrazo tautomerism that has been widely studied using IR and Raman (Pfeffer *et al.,* 1973), resonance Raman (Arenas *et al.,* 1997) and electron absorption and emission spectroscopies (Pierrat*et al.,* 2005).Pyridines like 2-methylpyridines that are most coarsely organized by the reaction of acetylene and hydrogen cyanide. 2-methylpyridine was the prime pyridine compound reported to be isolated in its pure form. It was basically isolated from coal tar in 1846 by Anderson. The derivatives of picoline have potent hypo lipidemic effects, anti-neoplastic and anti-inflammatory activities and exhibit better activity against leukemia and human glioma cell growth (Das *et al.,* 1992).

Many substituted pyridines are involved in bioactivities with applications in pharmaceutical drugs and agricultural products (Pierrat*et al.,* 2005; Jose and Mohan., 2005). The derivatives of pyrimidine and prodrugs are widely used for the treatment of neuronal damage which is caused by stroke. They also emphasize analgesics for acute and chronic pain, treatment for tinnitus, depression and even diabetic neuropathy. The picoline derivatives prepared from amino pyridine derivatives have shown to possess cholesterol lowering properties, anticancer and anti-inflammatory properties.

Amino pyridines are extensively used in pharmacological and medical applications. Some of them exhibit anesthetic properties and have been used as drugs for certain brain diseases (Okamoto *et al.,* 1997; Carmona *et al.,* 1993). 2-Aminopyridine tagged oligosaccharides have been widely used for sensitive qualitative and quantitative analysis by high performance liquid chromatography with fluorescence detection(Okamoto *et al.,* 1997), in preparation of cytidine analogs (Hildbrand*et al.,* 1997) and it is also immensely used as a reagent in analytical chemistry the ring

nitrogen of most pyridines that undergoes reactions such as protonation, alkylation and acylation. The harmonic frequencies of pyridine derivatives were calculated by several authors (Yamamoto *et al.,* 1980; Destexhe *et al.,* 1994).

The FT-IR and FT-Raman spectra of 2-methylpyridine-1-oxide have been recorded. These spectra have been interpreted employing the scaled quantum mechanical forcefield (SQMFF) methodology, by directly transferring the scale factors obtained for pyridine (Arenas *et al.,* 1997). To the best of the knowledge, neither quantum chemical calculations, nor the vibrational spectra of MAP have been reported. Therefore, in the recent research, FT-IR and FT-Raman spectral analysis of MAP have been recorded and evaluated by density functional theory (DFT) performed by B3LYP/6-31+G(d,p) basis set.

7.2 METHODOLOGY

The sample of the present compound 2-(Methyl amino)pyridine (MAP) was purchased from Sigma-Aldrich Chemical Company with a stated purity of 98% and it was used as such without further purification. KBr pellet technique is extensively used to prepare sample because of its nature in a solid state.The FT-IR spectrum of the sample was recorded in the region 4000-400 cm^{-1}on a Perkin Elmer FT-IR BX spectrometer calibrated using polystyrene bands. The FT-Raman spectrum of the sample was recorded using 1064 cm^{-1} line of Nd:YAG laser as excitation operating at 200 mW power with the adsorption wavelength in the region 3500–100 cm^{-1} on BRUKER IFS-66V model interferometer that are operated with an FRA-106 FT-Raman accessory.The reported frequencies were found to be precise and accurate with ± 1 cm^{-1} for FT-IR and FT-Raman spectroscopy.

7.3 COMPUTATIONAL DETAILS

The entire calculations were performed at density functional theory (DFT) level using Gaussian 09W program package (Frisch*et al.,* 2004), invoking gradient geometry optimization (Schlegel., 1982). We have utilized the gradient corrected density functional theory(Hohenbergand W. Koh**n**., 1964)with the three parameters of hybrid functional (B3) (Becke., 1993) for the exchange part and the Lee-Yang-Parr (LYP)

correlation function (Lee *et al.*, 1988), accepted as a cost efficient approach for the computation of molecular structure and vibrational frequencies of certain optimized structures. By combining the results of the Gauss view program (Frisch*et al.*, 2004) with symmetry considerations, vibrational frequency assignments were made with a high degree of accuracy. The standard scaling factor for the number is equal to 0.963.

Gaussian 09W program, which is used to calculate the Raman activities (S_i) converts into relative Raman intensities (I_i) with the subsequent relationship that are derived from the intensity theory of Raman scattering (*Keresztury et al., 1993; 2002*).

$$I_i = \frac{f(\nu_0 - \nu_i)^4 S_i}{\nu_i[1 - \exp(-hc\nu_i / KT)]} \tag{7.1}$$

Where v_0 is the laser exciting wave number in cm^{-1} (we have used the excitation wave number v_0 = 9398.5 cm^{-1}, which corresponds to the wavelength of 1064 nm of a Nd:YAG laser in the research work), v_i is the vibrational wave number of the i^{th} normal mode (cm^{-1}), while S_i is the Raman scattering activity of the normal mode v_i,f (is a constant equal to 10^{-12}) is a chosen general normalization factor for all peak intensities h, k, c and T that are Planck and Boltzmann constants, speed of light and temperature in Kelvin, respectively.

7.4 RESULTS AND DISCUSSION

7.4.1 Vibrational Assignment

The optimized structure is shown in Figure 7.1.Transformation of force field and the subsequent normal coordinate analysis including the least square refinement of the scale factors and computation of the potential energy distribution (PED) were performed on a PC with the MOLVIB program (version V7.0-G77) manipulated by Sundius (2002;1990). For the graphs of simulated FT-IR and FT-Raman spectra, pure Lorentzian band shapes were used with a band width of 10 cm^{-1}.

The MAP consists of 16 atoms and belongs to a C1 point group symmetry hence the number of normal modes of vibrations for this molecule has 42 normal modes of vibrations that are dynamic in both IR absorption and Raman Spectrum. There are 29

different mode of vibrations that are in-plane and the remaining 13 is out-of-plane with bending vibrations. The bands that fit in to the in-plane modes are depicted as A′ and the out-of-plane modes are represented as A″. The harmonic frequencies of the vibrations are depicted for MAP at B3LYP levels with the help of triple split valence basis set in along with the scattering and polarization functions with 6-31+G(d,p) basis set. FT-Raman and FT-IR frequencies for different mode ofvibrations are shown in Table 7.1. The experimental FT-IR and FT-Raman spectra in solid phase were shown in Figure 7.2 and Figure 7.3 along with calculated FT-IR and FT-Raman spectra by B3LYP/6-31+G (d,p) level.

7.4.2 C–H Vibrations

For all the aromatic compounds the C–H stretching vibrations are observed in the region 3100–3000 cm^{-1} (Varsanyi, 1974). In the present study, there were four adjacent hydrogen atom left around the ring and give rise to four C–H stretching modes, four in-plane bending and four out-of-plane bending vibrations which corresponds to modes C–H for the title molecule stretching vibrational bands that are observed at 3460 and 3200 cm^{-1} in FT-IR spectrum. The C–H in-plane bending and C–H out-of-plane bending vibrations are normally found in the range 1000–1300 cm^{-1} and 750–100 cm^{-1} in aromatic compounds (Karabacak *et al.*, 2008; Fereyduni*et al.,* 2011). The vibrational frequencies are assigned at 1350, 1160, 1170 and 1100 cm^{-1} for in-plane bending in FT-IR and FT-Raman spectra as they possess very strong intensities. The C–H out-of-plane bending vibrations are observed as medium, strong and very strong bands at 1020, 970 and 840 cm^{-1} in FT-Raman spectrum. The calculated wavenumbers supports the assignments at 1045, 965, 952 and 841 cm^{-1}.

7.4.3 CH_3 Group Vibrations

The MAP title molecule has CH_3 group in 2-positions, for the specific assignments of CH_3 group frequencies, with nine fundamentals that can be correlated to each CH_3 group namely the asymmetric stretching (in-plane and out-of plane hydrogen stretching modes), symmetric stretching, out-of-plane bending, in-plane bending, symmetric deformation, out-of-plane rocking in-plane rocking and distortion modes.

The C–H stretching in CH_3 takes place at lower frequencies than those of aromatic ring (3100–3000 cm^{-1}). The asymmetric C–H stretching mode of CH_3 group is expected around 2980 cm^{-1} and the symmetric one is expected in the region 2870 cm^{-1}.The asymmetric deformation of CH_3 group is usually observed at around 1450 cm^{-1} for methyl substituted aromatic rings and ultimately suits for the title compound. The asymmetric vibration of CH_3 produces bands that are observed at 3100 cm^{-1} in FT-IR spectrum as very weak band whereas the symmetric vibration of CH_3 is computed at 3011 cm^{-1}. As predicted in the literature, very weak band at 1270 cm^{-1} is assigned to CH_3 in-plane bending vibration while the medium band at 1190 $cm^{-1}$is assigned to CH_3 out-of-plane bending vibration in FT-Raman spectrum. The out-of-plane rocking vibration appears at 1000 cm^{-1} and 990 cm^{-1} in FT-IR and FT-Raman spectra with very strong and very weak intensities.

7.4.4 C-C Vibrations

The bands between 1650 and 1480 cm^{-1} are within theC–C stretching modes (Saravanan *et al.*, 2017). In the present study, the C−C stretching vibrations of the title compound was observed at 2900, 1620, 1490 and 1450 cm^{-1} in the FT-IR spectrum and 1450 cm^{-1} in FT-Raman spectrum. The out-of-plane and in-plane bending vibrations of C–C group are depicted in Table 7.1. These assignments are in good terms with the literature reviews(Sathyanarayana., 2004).

7.5 CONCLUSION

MAP have been characterized by FT-IR, FT-Raman spectra using B3LYP method 6-31+G (d,p) basis set. The assignments of the fundamental frequencies are confirmed by the qualitative agreement between the calculated and the observed frequencies.

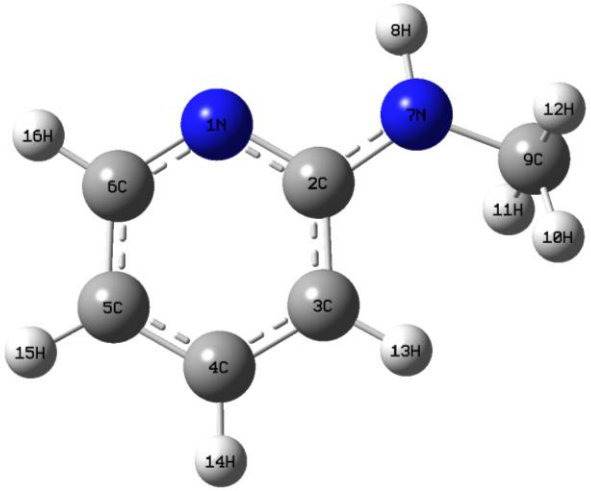

Figure 7.1 The optimized structure of MAP

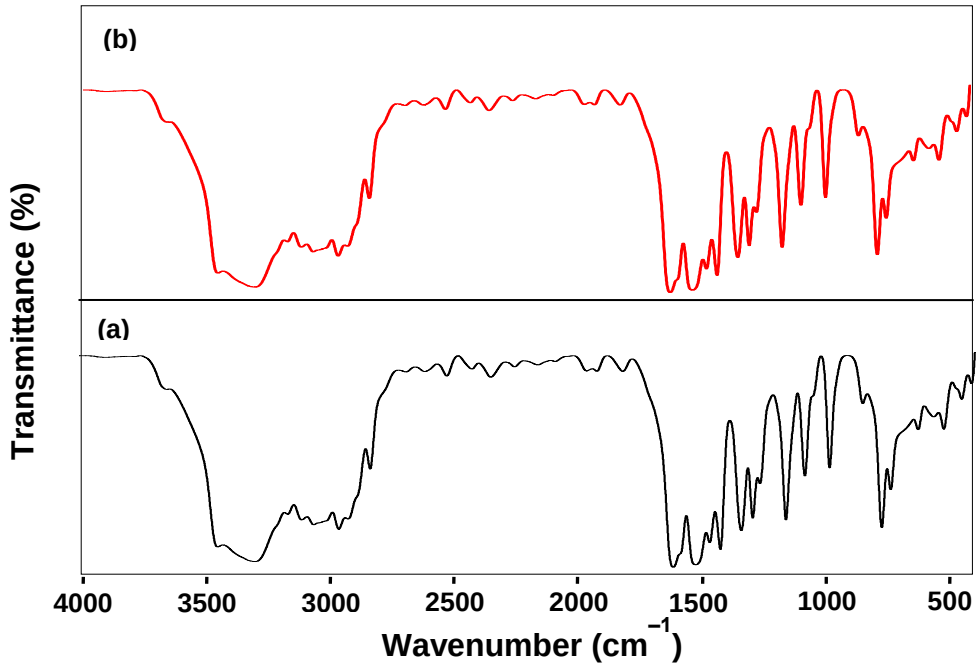

Figure. 7.2 Comparison of experimental and calculated FT-IR spectra of MAP: (a) experimental and (b) calculated with B3LYP/6-31+G(d,p).

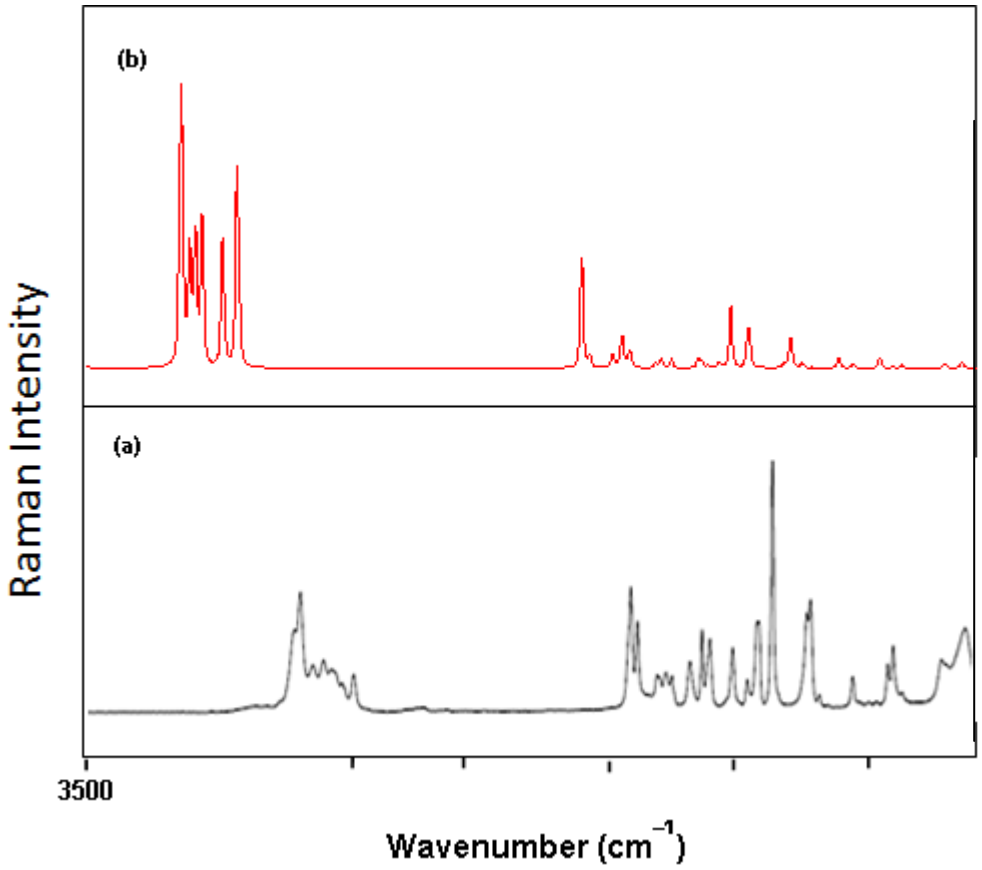

Figure 7.3 (a) The experimental FT-Raman spectrum of MAP

(b) The calculated FT-Raman spectrum of MAP

Table 7.1 Vibrational assignments of FT-IR and FT-Raman frequencies along with the theoretically computed (B3LYP/6-31+G(d,p)) wavenumbers and the percentage of potential energy distribution, IR intensities (Km mol^{-1}) and Raman intensities (Å^{o}amu^{-1}) are obtained for MAP.

Sl. No.	Experimental wavenumber (cm^{-1})		Calculated wavenumber (cm^{-1})		IR intensities	[a]Raman intensities	Assignments with % of PED[b]
	FT-IR	FT-Raman	Unscaled	Scaled			
1	3460(vw)		3446	3343	48.087	100.584	νCH(99)
2	3200(vw)		3218	3197	5.299	98.832	νCH(99)
3			3203	3175	21.538	71.568	νCH(98)
4			3185	3125	10.822	89.907	νCH(97)
5			3162	3102	25.938	84.467	CH_3asym(98)
6	3100(vw)		3135	3082	19.349	75.266	CH_3asym(95)
7			3054	3011	41.182	97.561	CH_3sym(91)
8	2900(vw)		2997	2953	82.975	86.601	νCC(72), νCH(63)
9	1620(s)		1648	1613	303.347	57.335	νCC(78), νNH(48), νCN(18)
10			1617	1592	44.552	6.476	νCN(67), βCC(45), νCH(28)
11	1550(s)		1558	1527	226.467	0.255	νCN(69), βCH(37), νCC(17)
12			1526	1509	6.952	7.654	νNH(63), CH_3sym(43), βNH(19)
13	1490(vw)		1494	1463	33.986	3.632	νCC(62), βCH(31), νCN(29)
14			1489	1456	11.215	15.167	νCN(59), CH_3asym(35)
15			1466	1438	25.772	5.424	νNC(82), νCH(33), νCC(15)
16	1450(m)	1450(s)	1456	1426	56.102	6.044	νCC(65), βCN(47), βCH(25)
17	1350(s)		1358	1332	53.650	3.052	βCH(66), νCC(24), βNC(21)
18			1336	1318	33.457	4.763	βCH(63),νCC(22), νNH(19)
19		1270(vw)	1296	1276	2.411	4.097	CH_3ipb(71), βCN(26), βCH(16)
20		1190(m)	1193	1183	12.776	4.337	CH_3opb(75), CH_3sym(22)
21	1160(vs)	1170(m)	1179	1136	12.104	3.924	βCH(59),νCC(22), νCN(16)
22			1153	1121	4.106	1.176	CH_3sb(58), βCH(31), CH_3ipb(26)
23	1100(vs)		1111	1093	3.448	2.314	βCH(43),νCC(22), βCN(16)
24			1099	1083	5.560	0.932	CH_3ipr(68), βNC(21)
25		1020(m)	1064	1045	7.099	27.564	γCH(57), tRsymd(42), νCC(22)
26	1000(vs)	990(vw)	995	972	8.474	25.288	CH_3opr(58), νCN(32), βCH(17)
27			983	965	0.012	0.567	γCH(56), Rtrigd(45), βNH(11)
28		970(s)	975	952	0.428	0.299	γCH(51), tRtrigd(34), Rsymd(19)
29		840(vs)	853	841	1.502	1.842	γCH(47), CH_3ipr(22),γCN(13)

Table continue …

Table continue…

30			828	912	3.050	18.193	βNH(51), γCN(23), CH_3opr(18)
31			783	771	52.895	2.212	Rtrigd(43),νCC(39),νNH(17)
32	750(s)	750(s)	746	732	18.018	0.145	Rasymd(49),γNC(38), CH_3ipb(11)
33	700(vw)		641	627	0.978	4.451	βNC(32), γCN(23), CH_3asym(17)
34		550(w)	584	573	8.322	1.629	Rsymd(49),βCN(23),γCH (18)
35	540(vw)	500(vw)	531	518	0.311	0.171	γCN(35), Rsymd(29), Rasymd(19)
36	490(vw)	490(vw)	499	476	12.134	4.038	tRtrigd(31),γCN(26), γCH(18)
37		430(m)	428	409	26.768	0.519	βCN(37), βNC(26), βNH(12)
38		350(vw)	391	385	72.271	1.160	tRsymd(30), βCH(24), Rsymd(17)
39			233	221	1.208	0.291	tRasymd(25), tCH3(13), γNC(11)
40			225	207	2.607	1.447	γNC(30),Rsymd(17),γNH(13)
41			158	142	0.839	2.144	γNH(36),tRasymd(18), γCH(11)
42			72	65	12.397	0.793	tCH_3(44)

The relative intensities of the experiments are abbreviatedthat includes: vs-very strong, s-strong, m-medium, w-weak, vw-very weak. R-ring, ν-stretching, asym-antisymmetric stretching, sym-symmetric stretching, ipb-in-plane bending, b-bending, opb-out-of-plane bending, sb-symmetric bending, opr-out-of-plane rocking, ipr-in-plan rocking, d t-torsion, -deformation, trig-trigonal. [a]Raman intensities normalized to 100. [b]Only contributions larger than 10% are given.